

## REFERENCES

- An, G., Ma, W., Sun, Z., Liu, Z., Han, B., Miao, S., Ding, K. Preparation of Titania/carbon nanotube composites using supercritical ethanol and their photocatalytic activity for phenol degradation under visible light irradiation, Carbon. 45 (2007): 1795-1801.
- Ando, Y., Zhao, H., Shimoyama, H., Sakai, G., Kaneto, K., Physical properties of multiwall carbon nanotubes, J. Organic Material. 42 (1999): 77-82.
- Argazzi, R., Iha, N.M., Zabri, H., Odobel, F., B, C.A. Desing of molecular dyes for application in photoelectrochemical and electrochromic devices based on nanocrystalline metal oxide semiconductors, Coordination Chemistry Reviews. 248 (2004): 1299-1316.
- Betra, R.C., Sears, A. Continuum models of multi-walled carbon nanotubes, Solids and Structures. 44 (2007): 7577-7596.
- Bikiaris, D., Vassiliou A., Chrissafis, K., Paraskevopoulos K.M., Jannakoudakis, A., Docoslis, A. Effect of acid treated multi-walled carbon nanotubes on the mechanical, permeability, thermal properties and thermo-oxidative stability of isotactic polypropylene, Polymer Degradation and Stability. 93 (2008): 952-967.
- Bwana, N.N. Improved short-circuit photocurrent densities in dye-sensitized solar cells based on ordered arrays of titania nanotubule electrodes, Current Applied Physics. 9 (2009): 104-107.

- Datsyuk, V., Kalyva, M., Papagelis, K., Parthenios, K., Tasis, D., Siokou, A., Kallitsis, I., Galiotis, C. Chemical oxidation of multiwalled carbon nanotubes. Carbon. 46 (2008): 833-840.
- Gratzel, M. Dye-sensitized solar cells, J. Photochem. Photobiol. A:Chem, 4 (2003):145-153
- Gratzel, M. Photovoltaic performance and long-term stability of dye-sensitized mesoscopic solar cell, C.R. Chimie. 9 (2006):578-583.
- Harris P.F. Carbon nanotubes and related structure, Cambridge university press. 1999.
- Hsiao, P.T., Wang, K.P., Cheng, C.W., Teng, H. Nanocrystalline anatase TiO<sub>2</sub> derived from a titanate-directed route for dye-sensitized solar cell, J. Photochem. Photobiol. A:Chem. 188 (2007): 19-24.
- Ito, S., Murakami, T.N., Comte, P., Liska, P., Gratzel, C., Nazeeruddin, M.K., Gratzel, M. Fabrication of thin film dye sensitized solar cells with solar to electric power conversion efficiency over 10%, Thin Solid Films. 516 (2008): 4613-4619.
- Kasuga, T. Formation of titanium oxide nanotubes using chemical treatments and their characteristic properties: Thin Solid Films. 496 (2006): 141-145.
- Kim, G.S., Seo, H.K., Godble, V.P., Kim, Y.S., Yang, O.B., Shin, H.S. Electrophoretic deposition of titanate nanotubes from commercial titania nanoparticles: Application to dye-sensitized solar cells, Electrochemistry Communications. 8 (2006): 961-966.
- Lai, W.H., Su, Y.H., Teoh, L.G., Hon, M.H. Commercial and natural dye as photosensitizers for a waer-based dye-sensitized solar cell loaded with gold nanoparticles, J. Photochem. Photobiol. A:Chem. 195 (2008): 307-313.

- Lao, C., Chuai, Y., Su, L., Liu, X., Haung, L., Cheng, H., Zou, D. Mix-solvent-thermal method for the synthesis of anatase nanocrystalline titanium dioxide used in dye-sensitized solar cell, Solar Energy Material & Solar Cells, 85 (2005): 457-465.
- Lee, G.W., Kim, J., Yoon, J., Bae, J.S., Shin, B.C., Kim, I.S., Oh, W., Ree, M. Structural characterization of carboxylated multi-walled carbon nanotubes, Thin Solid Films, xx (2007): xxx.
- Lee, K.M., Hu, C.W., Chen, H.W., Ho, K.C. Incorporating carbon nanotube in a low temperature fabrication process for dye-sensitized TiO<sub>2</sub> solar cells, Solar Energy Material & Solar Cells, xxx (2008):xxx-xxx.
- Lee, T.Y., Alegaonkar, P.S., Yoo, I.B., Fabrication of dye sensitized solar cell using TiO<sub>2</sub> coated carbon nanotubes, Thin Solid Film, 515 (2007):5131-5135.
- Lee, T.Y., Yoo, J.B. Adsorption characteristic of Ru(II) dye on carbon nanotubes for organic solar cell, Diamond & Related Materials 14 (2005): 1888-1890
- Ma, Y., Lin, Y., Xiao, X., Zhou, X., Li, X. Sonication-hydrothermal combination technique for the synthesis of titanate nanotubes from commercially available precursor, Material Research Bulletin, 41 (2006): 237-243.
- Nazeeruddin, M.K., Agelis, F.D., Fantacci, S., Selloni, A., Liska, P., Ito, S., Takeru, B., Gratzel, M., Combined Experimental and DFT-TDDFT Computational Study of Photoelectrochemical Cell Ruthenium Sensitizers, J. Am. Chem. Soc. 127 (2005): 16835-16847.

- Ngamsinlapasathain, S., Pvasupree, S. Dye-sensitized solar cell made of mesoporous titania by surfactant-assisted templating method, Solar Energy Material & Solar Cells. 90 (2006): 3187-3192.
- Ong, K.G., Varghese, O.K., Mor, G.K., Shankar, K., Grimes, C.A. Application of finite-difference time domain to dye-sensitized solar cells: The effect of nanotube-array negative electrode dimensions on light absorption, Solar Energy Material & Solar Cells. 91 (2007): 250-257.
- O'Regan, B., Gratzel, M. Low-cost high-efficiency solar cell based on dye-sensitized colloidal TiO<sub>2</sub> films, Nature. 353 (1991): 737-740.
- Ou, H.H., Lo, S.L. Review of titania nanotubes synthesized via hydrothermal treatment: Fabrication, modification, and application, Separation Purification Technology. 58 (2007): 179-191.
- Park, J.H., Alegaonkar, P.S., Jeo, S.Y., Yoo, J.B., Carbon nanotubes composite: Dispersion routes and field emission parameters, Composites Science and Technology. 68 (2008): 753-759.
- Pavasupree, S., Jitputti, J., Ngamsinlapasathian, S., Yoshikawa, S. Hydrothermal synthesis, characterization, photocatalytic activity and dye-sensitized solar cell performance of mesoporous anatase TiO<sub>2</sub> nanopowders, Material Research Bulletin. 43 (2008): 149-157.
- Shanmugaraj, A.M., Bae, J.H., Lee, K.Y., Noh, W.H., Lee, S.H., Ryu, S.H. Physical and chemical characteristics of multiwalled carbon nanotubes functionalized with aminosilane and its influence on the properties of natural rubber composites, Composites Science and Technology. 67 (2007): 1813-1822.

- Tsai, C.C., Nain, J.N., Teng, H. Mesopous nanotube aggregates obtained from hydrothermally treating TiO<sub>2</sub> with NaOH, Applied Surface Science, 253(2006): 1898-1902.
- Tsoukleris, D.S., Arabatzis, I.M., Chatzivasiloglou, E., Kontos, A.I., Belessi, V., Bernard, M.C., Falaras, P. 2-Ethyl-1-hexanol based screen-printed titania thin films for dye-sensitized solar cells. Solar Energy, 79 (2005): 422-430.
- Viriya-empikul, N., Sano, N., Charinpanitkul, T., Kikuchi, T., Tanthapanichakoon, W. A step towards length control of titanate nanotubes using hydrothermal reaction with sonication pretreatment, Nanotechnology, 19 (2008): 035601.
- Viriya-empikul, N., Charinpanitkul, T., Sano, N., Thongprachan, N., Soottitantawat, A., Kikuchi, T., Bureekaew, S., Tapanichakoon, W. Photocatalytic property of titanate nanostructures synthesized by hydrothermal process, J. Am. Chem. Soc. 327 (2007): 835-847.
- Wang, W., Serp, P., Kalck, P., Faria, J.L. Visible light photodegradation of phenol on MWCNT-TiO<sub>2</sub> composite catalyst prepared by a modified sol-gel method, J. Molecular Catalyst A: Chemical, 235 (2005): 194-199.
- Xia, X.H., Jia, Z.J., Y., Liang, Y., Wang, Z., Ma, L.L. Preparation of multi-walled carbon nanotube supported TiO<sub>2</sub> and its photocatalytic activity in the reduction of CO<sub>2</sub> with H<sub>2</sub>O, CARBON, 45 (2007): 717-721.
- Yang, J., Jin, Z., Wang, X., Li, W., Zhang, J., Zhang, S., Guo, X., Zhang Z. Study on composition, structure and formation process of nanotube Na<sub>2</sub>Ti<sub>2</sub>O<sub>4</sub>(OH)<sub>2</sub>, Dalton Trans. 1 (2003): 3898-3901.

# APPENDIX

## Publications Resulting from This Research Work

### National Proceedings

1. P. Lorturn, S. Sangkaew, G. Grehan, and T. Charinpanitkul, "Extinction of Solar Energy due to the Presence of fog Droplets Emerging Colase to Collector Surface" Proceeding of the 56<sup>th</sup> RGJ Seminar Series: CHEMICAL ENGINEERING SCIENCE AND TECHNOLOGY, September 28, 2007, Bangkok, Thailand.
2. P. Lorturn, N. Viriya-empikul, G. Tumcharern, W. Tanthapanichakiin, and T. Charinpanitkul, "Investgation of DSSC Electrodes Prepard from Titanate Nanotube-Carbon Nanotube Composite" *Proceeding of the 12<sup>th</sup> Asian Pacific Conference of Chemical Engineering Congress* August 4-6, 2008, Thailand.
3. P. Lorturn, N. viriya-empikul, A. Soottitantawat, G. Tumcharern, W. Tanthapanichakoon and T. Charinpanitkul. "A TWO-STEP HYDROTHERMAL METHOD FOR PREPARING TITANIA NANOSTRUCTURE WITH HIGH SURFACE AREA" *Proceeding of 8<sup>th</sup> IEEE Conference on Nanotechnology*", August 18-21, 2008, Texas, USA.

## Extinction of solar energy due to the presence of fog droplets emerging close to collector surface

### Abstract

The one cause of solar cell efficiency lost is the obstruction that attenuate the sun light going to solar cell. Fog is one of obstruction which is in the form of small droplet. The absorption and scattering reduces the intensity of sun light before goes through the solar cell. Size and size distribution of fog's droplet will give exactly information about losing intensity that effect to solar cell efficiency. The computation program has been developed to explain relation of size and size distribution to intensity of light by using Beer-lamber law. The Beer-lamber law will describes their relation in term of extinction coefficient ( $C_{ext}$ ). Measurements are also possible by turbidimetry technique which is also based on Beer-lamber law. Then, the artificial fog has been generated to compare with computation program. The result gives that the intensity of light is reverse proportional with density of droplet.

### Introduction

Solar cell is an important source of renewable energy. There are many factors that effect to solar cell efficiency, such as producing technology, producing material, the receiving light angle and surrounding environmental. Surrounding environmental includes smoke and smog from the pollution, rain and fog from the weather. All of these particles can obstruct the sun light because of scattering and absorption by particle which depend on size and refractive index. Refractive index has two parts, imaginary part effects to absorption and real part effects to scattering and reflection.

Dyed sensitized solar cell, which is one kind of solar cell, is generated photon by photo synthesis. Dense fog reduces solar radiation that effects to plant photosynthesis (Eugester et al., 2006). So, this research concentrates on fog and its droplet that reduce the efficiency of solar cell. Fog will be defined when horizontal visibility is less than 1 km. Therefore, it is important to know relationship between density of fog and intensity of light to explain how it reduces sun light. The main objective is to find relationship of size and size distribution that effect to intensity of light.



The principle of turbidimetry is measuring the decreasing of the intensity of light crossing a cloud of droplets at several wavelength to measure size distribution. Turbidimetry is proportional to extinction and density of particles.

The extinction consists of two parts. One is scattering and reflection of light from particles, the other is absorbing light inside particles. This technique uses to measure small particle with  $\frac{\lambda}{20} \leq d \leq 20\lambda$ , where  $d$  is particle diameter and  $\lambda$  is wavelength. Source or incident light, with its own intensity and wavelength spectrum, goes through empty air to the detector. The detector will receive the same incident light intensity or  $I_0$  (show figure 1.1) . If particles have been generated in the air between light source and detector, light intensity will be changed. Because the light will lost from reflection and scatter inside particle due to refractive index of particle, besides this it will be lost in term of absorption inside the particles. All of these are called  $I_{loss}$ . So, the new light intensity, that goes through the detector, should be  $I_0 - I_{loss}$  or  $I$  (show figure 1.2).

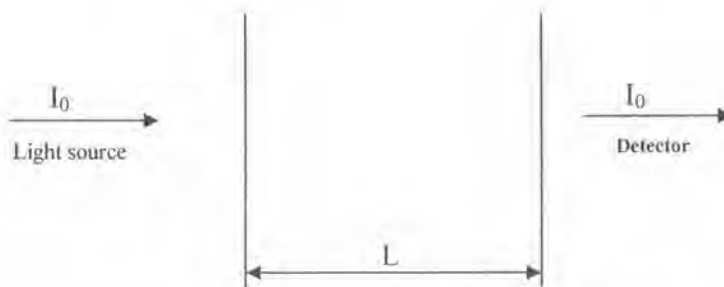


**Figure 1.1** The beam goes through without droplet

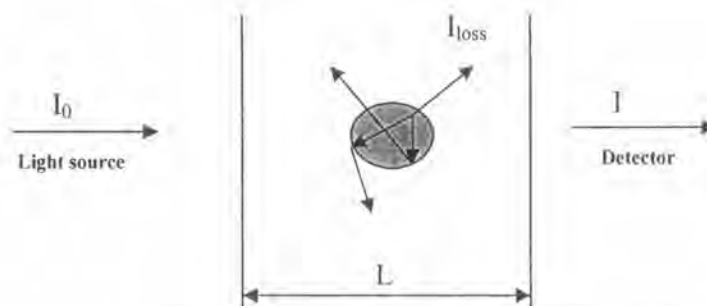


**Figure 1.2** The beam goes through with droplet

The relationship between beam intensity and wavelength can be calculated to size and size distribution from Beer-lamber law;

For one particle

$$\frac{I}{I_0} \Big|_{\lambda} = e^{-C_{ext}(d,n,\lambda)L} \quad \text{or} \quad \ln \frac{I}{I_0} \Big|_{\lambda} = -C_{ext}(d,n,\lambda)L \quad (1)$$

For several particles

$$\frac{I}{I_0} \Big|_{\lambda} = e^{-L \sum_{i=0}^n N_i C_{ext_i}(d_i, n, \lambda)} \quad \text{or} \quad \ln \frac{I}{I_0} \Big|_{\lambda} = -L \sum_{i=0}^n N_i C_{ext_i}(d_i, n, \lambda) \quad (2)$$

Which  $I \Big|_{\lambda}$  is intensity of beam after pass particles.

$I_0 \Big|_{\lambda}$  is intensity of incident light.

$N_i$  is number of particles of diameter  $d_i$ .

$L$  is path length of beam.

$C_{ext_i}$  is extinction coefficient of particle of diameter  $d_i$ .

$n$  is refractive index.

$\lambda$  is length of incident wavelength.

From equation (1) and (2),  $I \Big|_{\lambda}$ ,  $I_0 \Big|_{\lambda}$  and  $L$  from experiment give result in term of  $C_{ext_i}$  which give particle diameter. Because  $C_{ext_i}$  relates with particle diameter, incident wavelength and refractive index of particle. Light source emits a spectrum of wavelengths and from the particle material gives information of refractive index. Then, the objective is to extract the size distribution from the attenuation of the light spectrum.

The different shape graphs in figure 2 show effect of particle size, for one particle, to  $C_{ext_i}$  when particle diameter change 0.1, 1, 10 and 30  $\mu\text{m}$ , respectively, The graph shape is more fluctuant and  $C_{ext_i}$  increase with particle diameter.

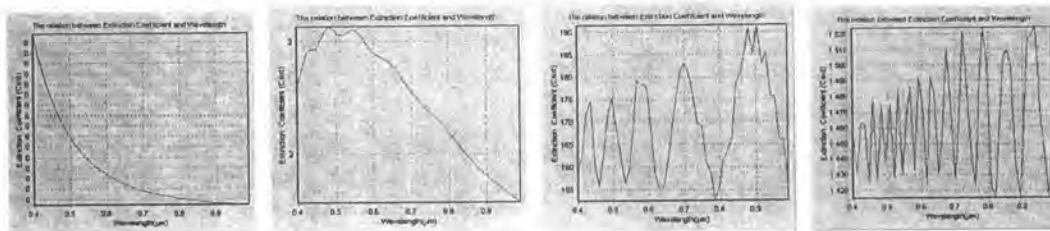


Figure 2 Particle size is 0.01, 1, 10 and 30  $\mu\text{m}$ .

The example of effect of particle size distribution, for several particles, to  $C_{ext_i}$  when rms is 0.5, 1, 5 and 10, respectively show in figure 3.  $C_{ext_i}$  increase with rms.

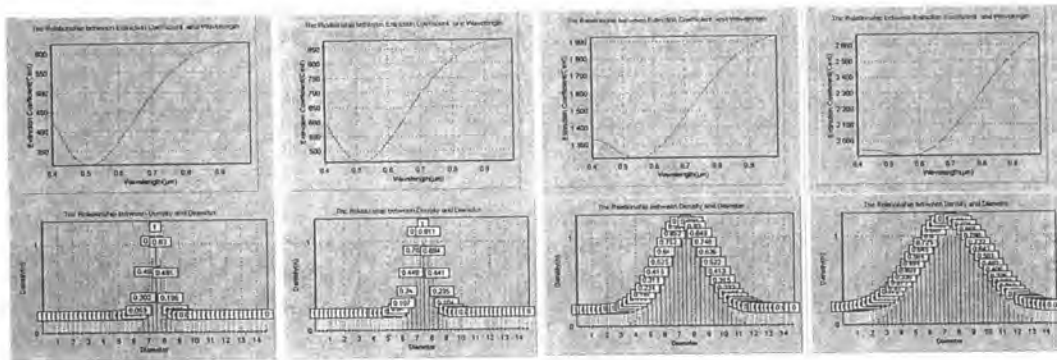


Figure 3 Rms is 0.5, 1, 5 and 10.

There are two step of this experiment. At first, the computation program has been developed to explain the relation by using turbimetry principle. Then, the developed computation program will be compared with artificial fog which are generated by ultrasonic nozzle.

### Experiment

The Delphi program source code is developed by using Beer-lamber law's to explain the relationship between intensity of light and size distribution of particle. There are many input parameters, maximum diameter, minimum diameter and average diameter and root mean square of particle, imaginary part of refractive index, real part of refractive index of medium, maximum wavelength and minimum wavelength of source light.  $C_{ext}$  is developed by fortran that also relates with diameter and refractive index of particle and wavelength of incident light. The result is needed in form of  $\ln \frac{I_0}{I}$ , so, Beer-lamber law use to find the relationship with  $C_{ext}$ .

Assume 
$$C_{ext} = L \sum_{i=0}^n N_i C_{ext_i}$$

So, 
$$\frac{I}{I_0} = e^{-C_{ext}}$$

$$\frac{I_0}{I} = \frac{1}{e^{-C_{ext}}}$$

$$\log \frac{I_0}{I} = \log \frac{1}{e^{-C_{ext}}}$$

The program is show in figure 3

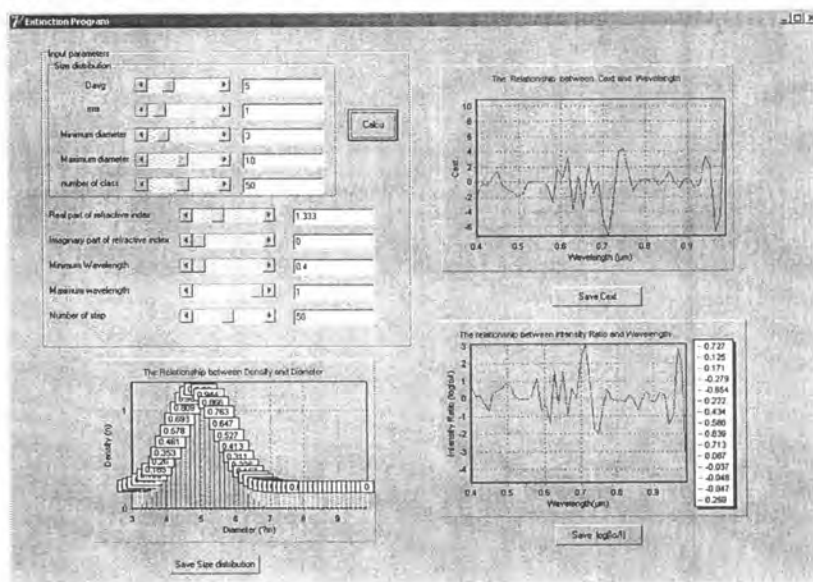
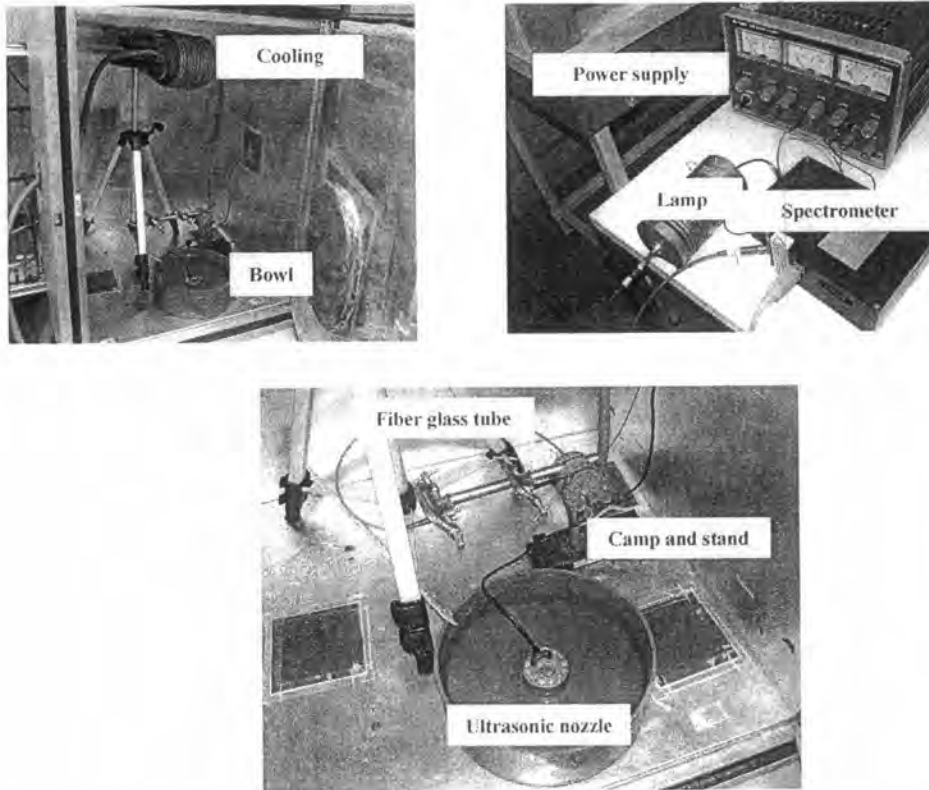


Figure 3

After that, source code is compared with artificial fog that generates inside the box. These are the apparatus that use to generate artificial fog, power supply, lamp, two fibre glass tubes, spectrometer, ultrasonic nozzle, cooling water, bowl, camp and stand(show in figure 4).



**Figure 4**

Setting the apparatus inside box (figure 4), the artificial fog is generated by increasing humidity inside box by ultrasonic nozzle which is put in the bowl with water and cooling water is opened to, reduce the temperature inside the box, help keeping fog. Measuring intensity of fog is varied with time. The camp and stand use to be handle opposite two fiber glass tubes which are opposite each other with  $L$  length. One is receiving light from lamp that generate from generator 5 volt and its wavelength is 400-900 nm. The other one will receive the light after go through the length  $L$  and send it to spectrometer. Spectrometer transform wavelength of white light to be a signal. At first, intensity is measured from empty air with intensity  $I_0$ . Then, intensity is measured after generate fog by ultrasonic nozzle between two fiber glass tubes with intensity  $I$ . Measure the intensity of light every 5 minute until 50 minute. The Ooibase program is used to show the raw data from experiment (show in figure 5).

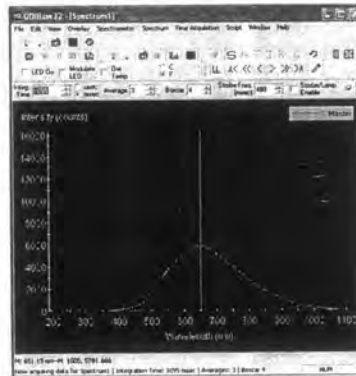


Figure 5

The raw data from Ooibase program is transformed to intensity ratio by program (shown in figure 6) before putting it into Turace 4.15 to get size and size distribution.

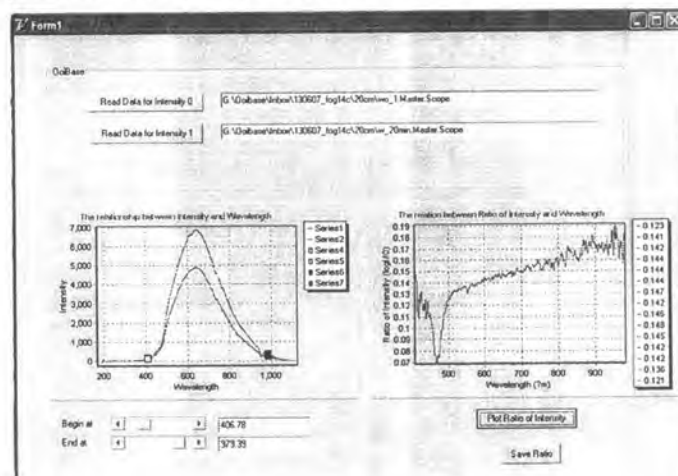


Figure 6

The data is obtained as intensity ratio and then processed through the program that transforms it into size and size distribution (shown in figure 7).

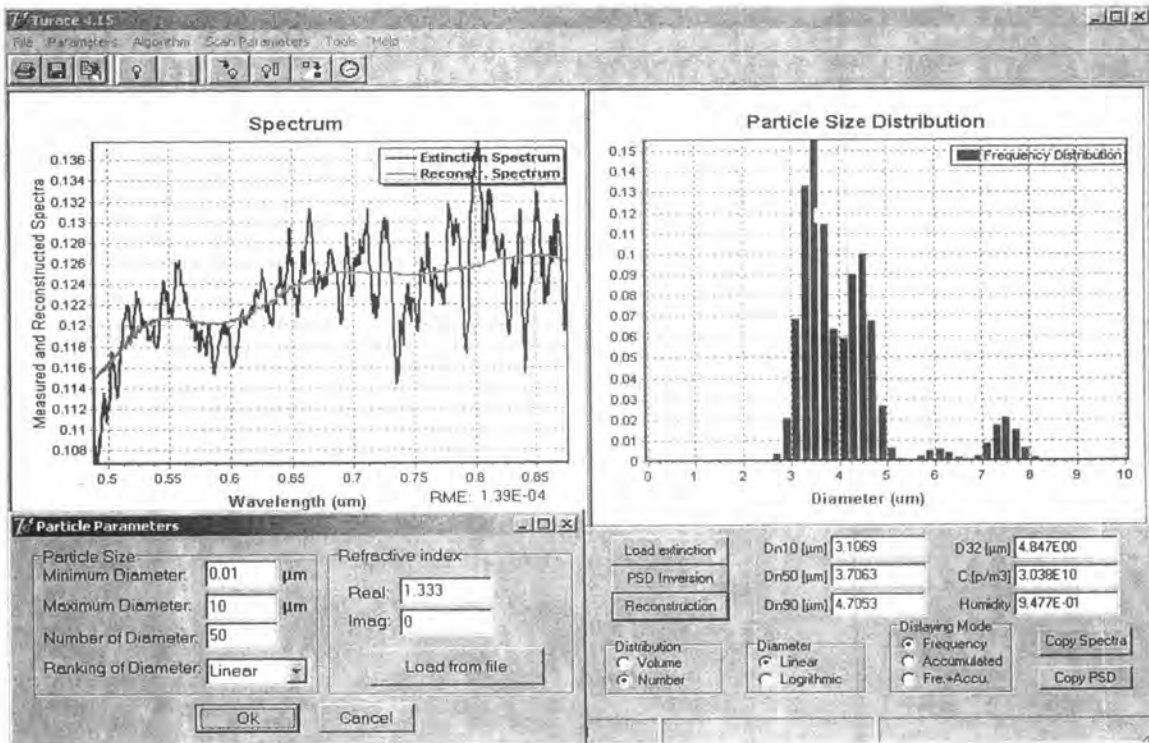


Figure 7

In this program can convert the ratio of light intensity to particle size and particle size distribution. Dn10 show diameter that 10 percent of the particle will be less than this, Dn50 shows diameter that 50 percent of the particle will be less than this or it is the mean diameter, Dn90 shows diameter that 90 percent of the particle will be less than this, and D32 is sauter mean diameter which is ratio between volume and surface of sphere. It is used to show average particle size in fluid dynamic.

Turace 4.15 has not been completely developed yet. Its limited is shown by direct computation. Found that, it gives a result when particle diameter is not more than 10  $\mu\text{m}$ . The graph in figure 8 shows computation result when particle is less than 1  $\mu\text{m}$ . The red curve presents real diameter which is 0.24  $\mu\text{m}$  and the blue curve presents computation diameter which is 0.25  $\mu\text{m}$ .

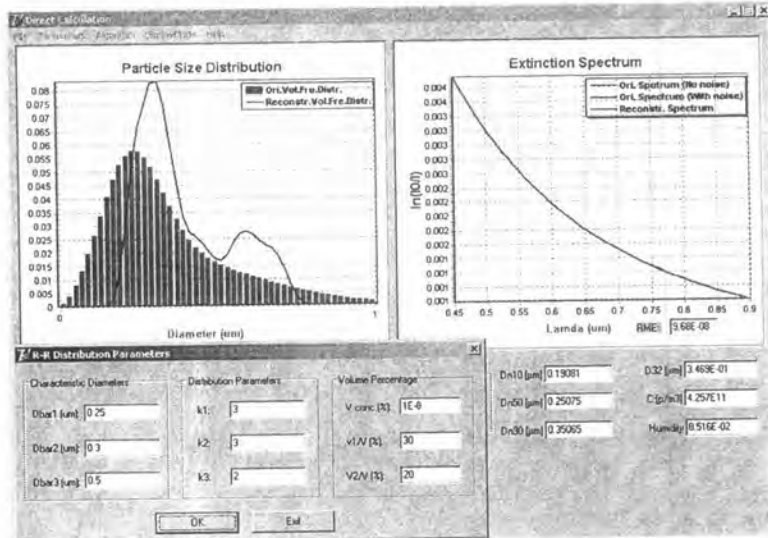


Figure 8

The graph in figure 9 show computation result when particle is less than 1  $\mu\text{m}$ . The red curve presents real diameter which is 5  $\mu\text{m}$  and the blue curve presents computation diameter which is 4.5  $\mu\text{m}$ .

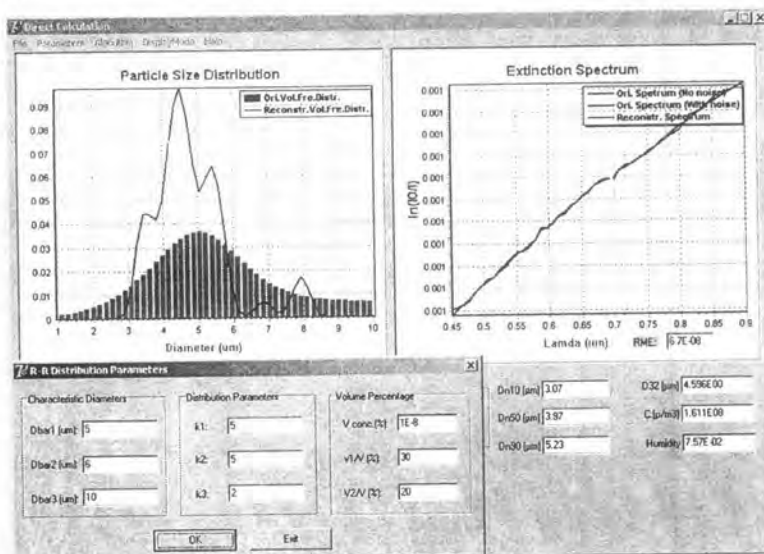


Figure 9



## Result and discussion

For computation program, the effect of size and size distribution to extinction coefficient ( $C_{ext}$ ) describe intensity of fog. Assume media is water and no absorption, its real part refractive index is 1.333 and imaginary part of refractive index is zero. At first, the computation program for one particle is considered. The relation between  $C_{ext}$  and wavelength is shown in the graph in figure 8. Wavelength is  $0.55 \mu\text{m}$  and particle diameter is 0.3, 1 and  $10 \mu\text{m}$ , respectively. The extinction coefficient is 0.032, 3.09 and 166, respectively. The bigger particle cause many time scattering inside its particle more than smaller particle. So, light intensity is attenuated before reach the detector.

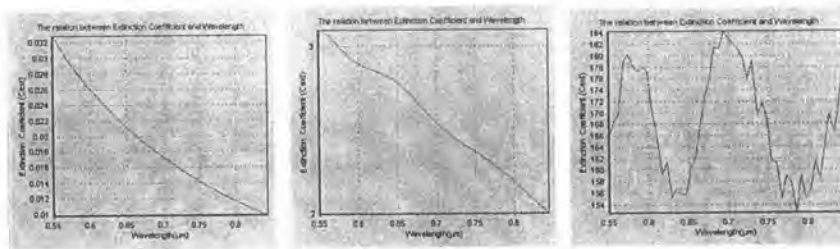


Figure 8

For several particles, The relation between  $C_{ext}$  and wavelength is shown in the graph in figure 9. The average particle diameter is 0.3, 1 and  $10 \mu\text{m}$ , respectively.  $C_{ext}$  is increase when particle is bigger.

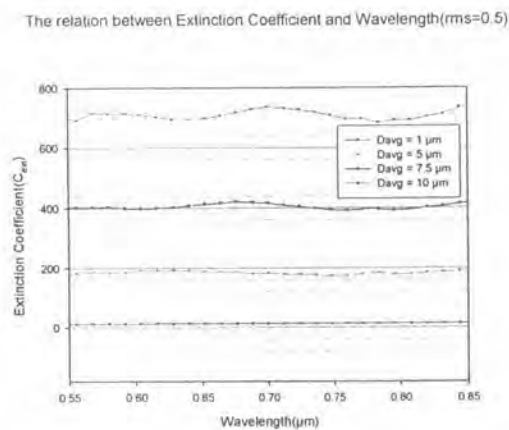


Figure 9.1

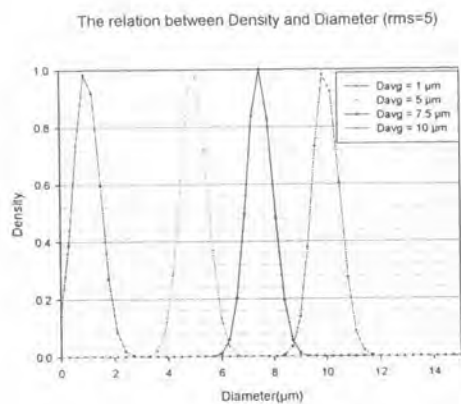


Figure 9.2

Consider term of distribution for several particles, in figure 10 show different rms, 0.1, 1, 5 and 10, respectively. When particle diameter distribution is increase, light intensity is more attenuant.

The relation between Extinction Coefficient and Wavelength (Davg=0.75μm)

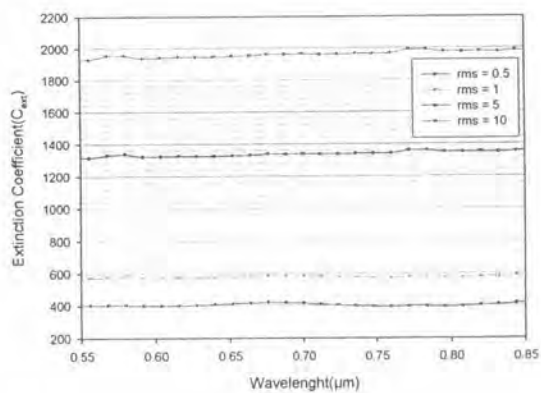


Figure 10.1

The relation between Density and Diameter (Davg=7.5μm)

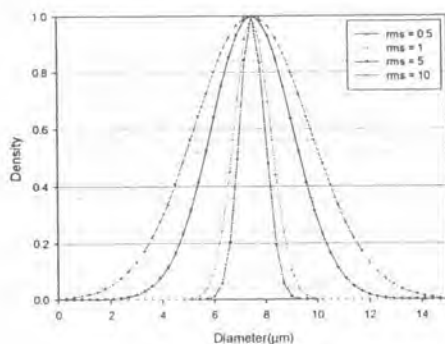
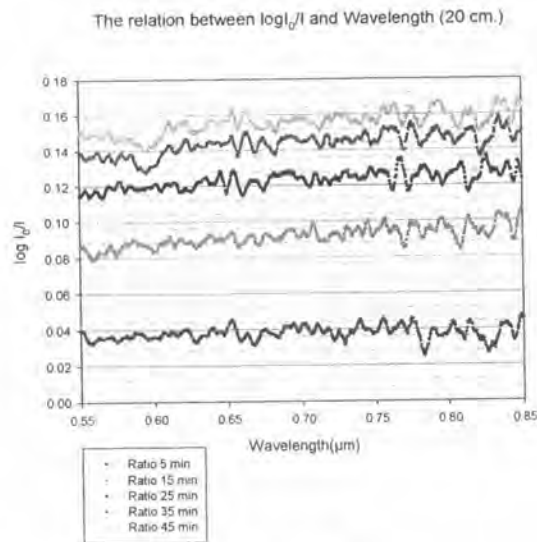


Figure 10.2

For experiment part

The fog intensity is measured by varying time of generating fog. Normally, fog intensity increase with time, but, light intensity at detector decrease with time. The relation between  $\log I_0/I$  and wavelength in figure 10. Generating fog time is 5 minute, gives the least ratio of  $\log I_0/I$  and wavelength. The ratio of  $\log I_0/I$  and wavelength increase with time until 45 minute. Because fog intensity increases with time to generate fog . The detector will receive less intensity of light with increasing time,  $I_0 > I_{5\text{min}} > I_{15\text{min}} > I_{25\text{min}} > I_n$  when time = 0 to n.

So ratio is  $\frac{I_0}{I_{5\text{min}}} < \frac{I_0}{I_{15\text{min}}} < \frac{I_0}{I_{25\text{min}}} < \frac{I_0}{I_n}$ . Then,  $\log \frac{I_0}{I_{5\text{min}}} < \log \frac{I_0}{I_{15\text{min}}} < \log \frac{I_0}{I_{25\text{min}}} < \log \frac{I_0}{I_n}$ .



**Figure 10**

From Turace 4.15 found that the size of artificial fog is  $1.913 \mu\text{m}$ . The graph in figure 11 shows relation between  $D_{n50}$  or mean size diameter and time. The diameter nearly constant with time. And figure 12 show relation between concentration and time. The concentration of particle increases with time.

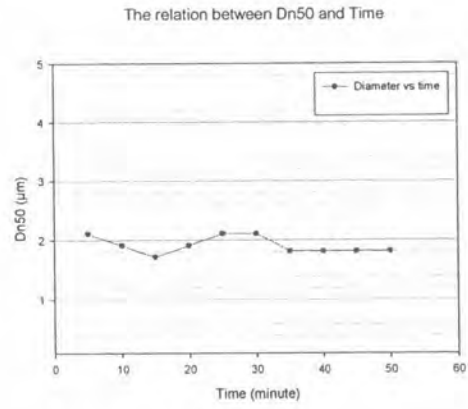


Figure 11

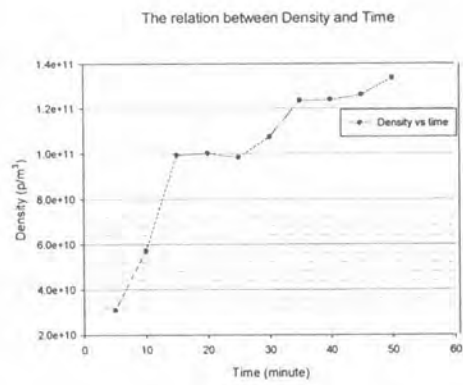


Figure 12

**Conclusion**

Fog is a small droplet which can reduce solar cell efficiency by obstruct sun light intensity by itself refractive index. The computation program shows relation of density of fog and light intensity by turbidimetry that  $C_{\text{ext}}$  increase with particle diameter and particle diameter distribution. For the experiment with artificial fog in the box, found that the size is nearly constant while the concentration increases with time.

## VITA

Miss Patcharaporn Lorturn was born on June 3<sup>rd</sup>, 1984 in Lampang province, Thailand. She studied elementary school at Tripop Wittaya school, and secondary school at Boonyawat Wittayalai School. In 2006, she received the Bachelor Degree of Science (Chemical Technology) from Chulalongkorn University. After that, she gained admission to Graduate School of Chulalongkorn University and she graduated in 2008 with the thesis entitled "Titania - Carbon Nanotubes Composite for Dye Sensitized Solar Cell Application".

